DEPLETION OF NEAR-CRITICAL OILS: COMPARISON BETWEEN PORE NETWORK MODEL PREDICTIONS AND EXPERIMENTAL RESULTS

N. Piccavet (1), J. Long(1), G. Hamon(1), I. Bondino(2), S. McDougall(3)
(1) TOTAL (2) TOTAL UK E&P (3) Heriot Watt University Edinburgh

This paper was prepared for presentation at the International Symposium of the Society of Core Analysts held in Trondheim, Norway 12-16 September, 2006

ABSTRACT

Literature data show a wide scatter in critical gas saturation when near-critical oils are depleted. Some controls have clearly been identified, such as the depletion rate, but cannot explain such a large scatter. In fact, the influence of several other parameters is still unclear. This paper sets out to study the effects of rock characteristics, core height and presence of initial water saturation, and the influence of the corresponding capillary to gravity ratios on critical gas saturation for solution gas-drive.

The combination of three different approaches has been used to decipher the variability:

1. Firstly, pore network simulations have been performed to assess the influence of rock properties and Swi and design the experiments
2. Secondly, to check the validity of the pore network model predictions, several depletion experiments were performed with the same fluid (C1/C10) at 38°C and 400 bars initial pressure. During the depletion at 4 b/d depletion rate, fluids were recovered and measured at high pressure. In-situ saturation monitoring ensured a good control of saturation gradients within the cores.
    - The depletion behaviour of a 750 mD homogeneous sandstone is compared with a 4 mD rock.
    - The depletion performance of a dry Berea sample is compared with a 26 % initial water saturation sample
    - The depletion behaviour of a high permeability, one metre long Berea core is compared with a 10 cm tall sample
3. Thirdly, numerical simulations with both pore network and ECLIPSE simulators were carried out and compared with experimental data.

It is concluded that:

- Both the rock characteristics and the amount of initial water saturation have a very significant effect on critical gas saturation and experimental observations are in agreement with predictions of pore network models
- Whilst there appears to be little evidence of the effect of core height on critical gas saturation, in-situ saturation profiles versus time and relative permeabilities are significantly affected. These issues are well described by the ECLIPSE simulations.

INTRODUCTION

Whereas the effects of pressure decline rate and gas/oil interfacial tension on critical gas saturation (Sgc) and microscopic performance of solution gas drive has been significantly documented, the influence of sample length, pore structure and initial water saturation (Swi) has received relatively little attention. A number of contradictory experimental observations have been reported. Abrall and Iffly (1973) found that a larger critical gas saturation developed when the core length was increased from 13 cm to 100 cm but questioned the effect of small scale heterogeneity on these experiments. From theoretical considerations, they also suggested that oil recovery by depletion should increase as permeability increases. Madaoui (1975) stated that a minimum core height for depletion experiments is required to ensure that gravity forces can exceed capillary forces and allow gas flow. A larger Sgc was obtained when the core was mounted horizontally in comparison to that resulting from a vertically orientated core. Other studies focused on the effect of core length on critical gas saturation, but gas injection was performed rather than solution gas drive [3, 4]. Madaoui also found that Sgc increases when initial water saturation increases from 0 to 32% and when core permeability increases. More recently, Kortekaas and Van Poelgeest (1991) concluded that permeability, when ranging from 230 mD to 1900 mD has no influence on critical gas saturation for near-critical oils.

The ratio of gas/oil relative permeability curves after critical gas saturation has long been derived directly from oil and gas productions versus pressure data, provided that the PVT properties and viscosities are known [6]. This method implicitly assumes a uniform gas saturation profile within the core, however, and this assumption has not been checked routinely in the past. Indeed, the use of in-situ saturation monitoring has highlighted that this assumption was often wrong. More recently, history matching of experimental productions and in-situ saturations with reservoir simulators has illustrated that the gas/oil Kr curves obtained by solution gas-drive might be low compared to those achieved by gas injection [7]. This result has been questioned and ascribed to improper representation of the boundary conditions [8]. Pore network modelling (PNM) has also been used extensively to understand the difference between relative permeabilities for internal and external gas drives [9] and have highlighted the influence of several parameters, including depletion rate and diffusion coefficient [10, 11].
In this paper, we present four experimental depletion tests of near-critical oils, aiming at evaluating the effect of core length, initial water saturation and rock quality. We also show the interpretation of two experiments with a reservoir simulator and compare the experimental results with predictions from corresponding pore network modelling simulations.

EXPERIMENTAL WORK

Apparatus

The composite cores were successively mounted in a core holder as described in the sketch shown in figure 1. Continuous data acquisition in real time (pressure, temperature, gas and oil flow rates) is performed. The dead volume between the outlet of the core sample and the visual cell was kept to a minimum to reduce time delay in production. A

visual cell collecting produced fluids at reservoir conditions also allows an accurate detection of the onset of gas production. Finally, saturation profiles were measured using in situ saturation monitoring techniques (gamma or X-ray attenuation).

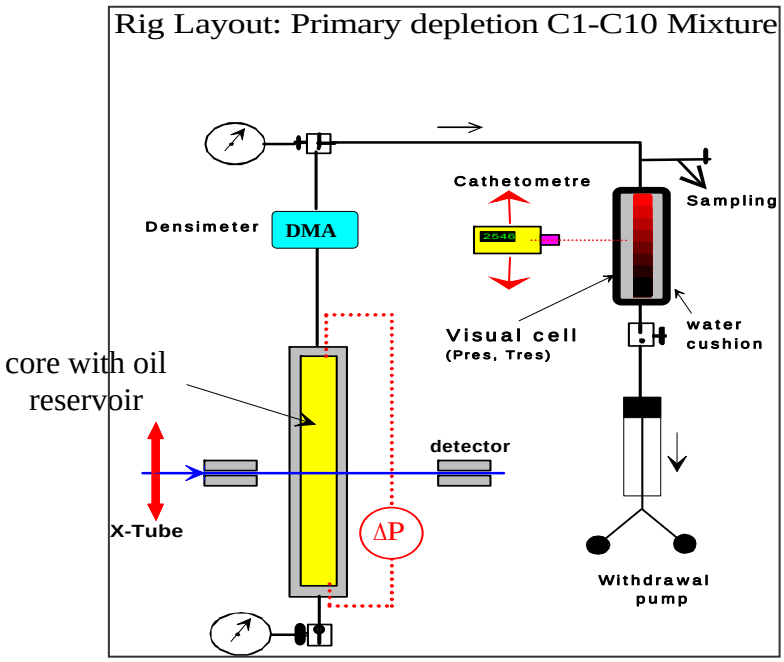

Figure 1

Core and fluid

Table 1 presents the characteristics of the outcrop sandstone cores used in this study. The oil used comprised a mixture of methane (80.43 %mol) and decane. The characteristics of the oil at bubble point pressure were Bo = 2 rm^3/sm^3, Psat = 341 bar, GOR = 471 sm^3/sm^3, µo =0.12 cP. These were verified by measurements (Bo, GOR, Psat) before the start of each experiment. Figure 2 shows the increase of gas/oil interfacial tension (IFT) as pressure decreases. The IFT of this near critical oil is very low at bubble point 0.1 mN/m.

Core preparation

The probe permeameter/X-ray CT scans confirm that the samples are homogeneous. For the first three experiments, the samples were saturated with C10 at laboratory conditions after their positioning in the core holder. The cores were then pressurized to reservoir conditions and flooded with the C1C10 mix. For the experiment incorporating irreducible water, the core was sequentially flooded with water, Marcol® oil to reach Swi, and toluene, and then pressurized to reservoir conditions and finally flooded with the C1C10 mix.

Depletion experiments

All depletion experiments were initiated at 38°C and 380 bars, 40 bars above the bubble point and stopped at 250 bars. The depletion rate was 4 bars per day (0.167 b/h) for all the experiments. In all cases, the depletion was conducted by continuously extracting

fluid from the top of the vertically oriented core while keeping the net confining pressure constant and equal to 430 bars.

Determination of critical gas saturations
To determine the critical gas saturation value, two (three for the first experiment) criteria were used:

(i) the sharp increase of production GOR above the solution GOR, indicating the mobility of free gas. The volume of gas used for the calculation of the GOR is measured in the visual cell and not directly at the outlet of the core. Consequently, the Sgc value is slightly over-estimated.

(ii) the variation of the differential pressure. As soon as some gas leaves the core, the differential pressure increases.

(iii) the decrease of density of produced fluid indicating the free gas production. Online fluid density was only measured for the first experiment.

NUMERICAL WORK

Numerical simulations with both the pore network and Eclipse simulators were carried out and compared with experimental data.

Eclipse simulations
The experiments are modelled using a one dimensional compositional simulation model (Eclipse 300). The core is represented by one hundred numerical blocks, vertically oriented, with the outlet at the top. A specific keyword activates the variation of surface tension with pressure (figure 2) leading to the variation of capillary pressure with surface tension (figure 3). To model the boundary at the top, an additional block is added to the numerical model, where relative permeabilities are straight lines and capillary pressures are zero. A well is located in this block. A total reservoir volume production rate is specified for the production well.

Firstly, the total reservoir volume production rate is reproduced to match the pressure depletion. Then, sensitivity runs are performed to identify the parameters having the strongest influence on simulated results. Once done, combinations of sensitive parameters are tested. Final matches correspond to combinations that enable good matching of in situ saturation profiles and oil and gas production.

Pore network simulations
A pore network model, originally developed by McDougall and Mackay (1998) and McDougall and Sorbie (1999), is used. This pore network simulator takes into account the fundamental physical steps of the depressurization process from the nucleation of bubbles, to their growth by diffusion and expansion, to the final stages of coalescence and production in the porous media. Furthermore gravitational and viscous forces are also accounted for with the possibility of bubble migration and break-up.
After the relevant PVT information is input into the simulator, the network is anchored to the rock sample using the methodology described in [13]. The adopted pores size distribution is a truncated normal

$$f(r) = N(R\max - r)(r - R\min)\exp\left[-\frac{(r-\bar{r})^2}{2\sigma^2}\right], \quad \text{Rmin} < r < \text{Rmax} \qquad (1)$$

The main anchoring results for the low and high permeability samples are summarized below:

	Rmin (m)	Rmax (m)	Pore connectivity Z	Pore length
Low perm.	0.15E-6	1.7E-6	5	44E-6
High perm.	1.0E-.6	30E-6	6	144E-6

Experimental porosity and permeability were also matched. For more details, the characteristics of the simulators have already been presented in [9][10][11][12].

At this point, pore network simulations were run in both 2D networks (for easy visual inspection) and in 3D networks (for quantitative estimates of Sgc). Here, to try to preserve the core scale balance between gravitational and capillary forces, the Bond number was increased by a core length related factor. Using this procedure the 2D simulations in Figure 14 were used to assess the difference in gas evolution between the low permeability P80 core and the highly permeable dry Berea sample, whilst Figure 15 compares the water wet Berea case to the dry Berea. 3D simulations were then run on similar water wet networks comprising 30X15X15 nodes (including more than 20,000 volume elements having a vertical dimension twice as long as the lateral dimensions). As for the definition of critical gas saturation, we use one of the approaches formalised in [14] in the case of invasion percolation with a gradient: the system reaches the critical gas saturation when gas reaches the top of the network.

Twelve different stochastic realisations of the pore size distribution given by (1) were generated for each of the "dry" (Swi=0), "wet" (Swi≠0) and low permeability cases. The resulting critical gas saturations and the number of bubbles nucleated in each case (Nbub) are shown in Table 2.

INFLUENCE OF CORE LENGTH

The experiments #1 and #2 were designed to assess the effect of the core length on the gas/oil relative permeability curves (see Table 1 for characteristics and results). The Sgc values are very close for the two experiments (Sgc1 = 3.3% and Sgc2 = 3.6%). These very low Sgcs are consistent with the very low resisting capillary forces at early depletion time for near critical oils due to the low IFT at about 0.1mN/m (see Figure 2).

Relative permeability curves are obtained by history matching of Experiments 1 and 2 with Eclipse 300. The most sensitive parameters are the critical gas saturation and the gas relative permeability. The Sgc values put into Eclipse are those derived from the experiments. The gas relative permeabilities are presented in Figure 12. Figures 4 and 5 display the history matches of oil production and gas oil ratios of experiments 1 and 2.
Figure 6 and 7 present the experimental in-situ gas saturation profiles obtained during the depletion experiments. After gas breakthrough, these figures show sharp gas fronts moving downwards on the one meter long core whereas flatter gas saturation profiles are observed on the ten centimetre long core.

To explain the differences between profiles between the short and the long cores, the ratios between the capillary forces and gravity forces required to achieve a given Sg over the total core length were calculated as a function of pressure and therefore IFT (Fig 8 & 9). At the core scale, the gravity forces largely exceed the capillary forces on the one meter core over the whole depletion range. On the other hand, capillary forces are weak compared to gravity forces at the early depletion time on the short 10-cm core but become predominant for larger depletions. In summary, the long core experiment appears to be gravity-dominated whereas the short core depletion appears more capillary-dominated, particularly at late times.

A strong gravitational effect enhances the segregation of gas in the 1 meter core and consequently leads to the formation of a gas cap, as observed by in-situ monitoring, whereas a displacement dominated by capillary forces results in a less pronounced saturation gradient. To check this hypothesis, an Eclipse simulation was performed on the one meter long core using a tenfold increase in capillary pressure. Figure 13 confirms the increased smoothing of the gas saturation profiles when capillary forces become predominant.

Figures 10 and 11 show the good agreement achieved between experimental and simulated gas saturation profiles, whilst Figure 12 indicates that the gas relative permeabilities derived from history matching are dependent on core height.

INFLUENCE OF PORE STRUCTURE

Comparisons between experiments 1/2 (Sgc=3.3/3.6%, core length=10/100cm, high permeability=740mD) and experiment 3 (Sgc=12%, core length=30cm, low permeability=4.5mD) suggest a very strong influence of rock quality on critical gas saturation. Although these experiments were carried out with the same fluid system at the same depletion rate, higher capillary forces prevent early upward migration of gas in the low permeability sample despite the very low initial IFT.

2D network simulations predict a larger gas saturation for the core with lower permeability. Figure 14 shows the comparison of gas saturation maps (in white) for the high and low permeability samples at the same depletion pressure. At this point in the depletion, gas has broken through at the top of the high permeability network, whereas the gas cluster is still growing in a compact manner in the low permeability system.

Subsequent 3-D-simulations reproduce the experimental trend very well (Table 2) — Sgc is predicted to be 11.0% in the low permeability P80 sample and 5.6% in the highly permeable Berea sample. The radii of the P80 sample are thirty times smaller than those in the Berea model and so capillary forces are much more important in the low permeability system.

INFLUENCE OF WATER

A comparison between experiment 1 (Sgc=3.3%, core length=100cm, dry core) and 4 (Sgc=7%, core length=44cm, Swi=26.8%) shows that the critical gas saturation is significantly larger in the presence of initial water. As we showed that the core length has

no impact on the critical gas saturation (Table 1), we can conclude that the difference in Sgc between experiments 1 and 4 can be mainly ascribed to the presence of the third phase. We can hypothesise that the water may suppress gas evolution by effectively reducing the connectivity of the hydrocarbon phase, thereby affecting both the nucleation potential of the system and the subsequent growth of bubbles [15]. This hypothesis was tested through PNM simulations.

2D simulations confirm a larger gas saturation for the network at Swi. Figure 15 shows the comparison of gas saturation maps (in white) with and without initial water saturation at the same depletion pressure. At this point in the depletion, gas has broken through at the top of the dry network but is still growing in a compact manner in the network at Swi.

The results of corresponding 3D-simulations are presented in Table 2. The experimental trend is well reproduced with the pore network model, where Sgc in the presence of water is larger (7.7%) than when water is absent (5.6%).

Pore network modelling highlights some interesting issues relating to the effect of water on Sgc. Contrary to expectations, the presence of a 26.8% initial water saturation is insufficient to suppress gas evolution. Figure 16 shows that gas displaces large oil-filled pores in both cases, as evidenced by the range of pores occupied by gas at gas breakthrough (Figure 16).

The difference in the simulated Sgc values in systems with and without water is likely to be linked to the bubble density (Table 2): the mean density of bubbles at the end of simulations is 96 bubbles in networks containing water and 76 bubbles without water, due to a higher supersaturation when water is present. The effect of water on supersaturation was commented recently in the micromodel results of Nejad and Danesh [15], who compared depletion in virgin oil and water flooded systems and found an increase in bubble density by an order of magnitude in the second: water contains far less dissolved gas and so the process of diffusion of gas through water is comparatively slow, as the gas concentration gradients remain almost negligible throughout a depletion. As far as the modalities of diffusion are concerned, their conclusions between the waterflooded and the virgin case also apply here to explain the difference in bubble density between the wet and the dry cases: as water saturation increases diffusion pathways become longer and longer and supersaturation increases. As a consequence, oil may become more supersaturated in the presence of water in the same way as oil in a less connected system is more supersaturated than in a well connected one.
Additionally, at the same pressure below bubble point, the size of the bubbles is smaller when water is present as less dissolved gas is available and more bubbles are competing for this. As a result, gravitational forces have only a minor effect upon bubble growth and this also explains the higher Sgc.

Therefore, the result of the fourth experiment is also predicted by the pore network model, showing that the higher critical gas saturation observed in the presence of water is likely to be due to higher bubble density and reduced bubble size rather than suppression of growth. In fact, in water-wet systems, percolation arguments would suggest that Sgc

should be identical with or without Swi, assuming bubbles nucleated in the same oil-filled pores in both cases.

DISCUSSION

A comparison of experiments 1, 2 and 4 shows significant differences with core length. Very little oil is produced after gas breakthrough despite the very low initial IFTs. The average Sg versus pressure observed in these experiments at late depletion time resembles PVT data confirming the difficulty to expel oil and gas from the core. Finally, the comparison of experiments 1, 2 and 4 confirms that in situ Sg versus time is strongly constrained by the outlet boundary effect at the top of the core. All these observations suggest that a proper representation of the outlet boundary condition is required to history match gas oil depletion experiments as suggested by Goodfield and Goodyear [8]. On the other hand, the very low gas relative permeabilities obtained by history matching might represent flows of dispersed gas due to a very large number of bubbles. This high bubble density might be related to the very low initial IFT.

The influence of pore structure and initial water saturation on critical gas saturation is well predicted by pore network modelling confirming the predictive capability of this technique.

CONCLUSIONS

- 4 depletion experiments of near critical oils have been presented.
- Both the rock characteristics and the amount of initial water saturation have a very significant effect on critical gas saturation and experimental observations are in agreement with predictions of pore network models developed by McDougall and co-workers [12] [13].
- There is no evidence of an effect of core height on critical gas saturation, but a strong effect on in-situ saturation profiles versus time and gas-oil relative permeability are observed. Both of these are well described by the ECLIPSE simulations.

ACKNOWLEDGEMENTS

We wish to thank Total for its permission to publish this work. We are also especially grateful to JP Chaulet, M.N'Guyen for the experimental work.

REFERENCES

[1] Abgrall, E. and Iffly, R.: "Etude physique des écoulements par expansion des gaz dissous" , Revue de l'institut français du Pétrole, Sept-Oct 1973, Vol XXVIII n°5.73031, pp. 667-692.
[2] Madaoui, K. : « Conditions de mobilité de la phase gazeuse lors de la décompression d'un mélange d'hydrocarbures en milieu poreux » PhD thesis Toulouse University, France 1975
[3] Closmann, P.J.: "Studies of critical gas saturation during gas injection" SPERE August 1987
[4] Dumore, J.M.: " Development of gas saturation during solution gas-drive in an oil layer below a gas cap" SPEJ, sept. 1970
[5] Kortekaas, T.F., Van Poelgeest F.: " Liberation of Solution gas during pressure depletion of virgin and watered-out oil reservoirs" SPERE, Aug. 1991, 329-335

[6] Arps, J.J and Roberts, T.G.: " The effect of the relative permeability ratio, the oil gravity and the solution gas-oil ratio on the primary recovery from a depletion type reservoir" Trans. AIME, vol 204, 120-127, 1955.
[7] Egermann, P. and Vizika, O.: "A new method to determine critical gas saturation and relative permeability during depressurization in the near-wellbore region" SCA 2000-36, Abu Dhabi.
[8] Goodfield, M. and Goodyear, S.: "Relative Permeabilities for post-waterflood depressurisation" SPE 83958, Offshore Europe 2003, Aberdeen, UK, Sept. 2003
[9] Poulsen S., McDougall, S.R., Sorbie, K. and Skauge, A.: "Network modelling of internal and external gas drive" SCA 2001-17, Edinburgh, UK
[10] McDougall, S.R. and Sorbie, K.S.: "Estimation of critical gas saturation during pressure depletion in virgin and waterflooded reservoirs", Petr. Geosc, vol. 5, pp. 229-233, 1999.
[11] Bondino, I., McDougall, S.R. and Hamon, G: "Pore network modelling of heavy oil depressurisation: a parametric study of factors affecting critical gas saturation and 3-phase relative permeabilities", SPE Journal, June 2005
[12] McDougall, S.R. and Mackay, E.J.: "The impact of pressure-dependent interfacial tension and buoyancy forces upon pressure depletion in virgin hydrocarbon reservoirs", Trans IchemE, vol. 76, part A, pp. 553-561, 1998
[13] McDougall, S.R., Cruickshank, J. and Sorbie, K.S.: "Anchoring methodologies for pore scale network models: application to relative permeability and capillary pressure prediction", SCA 2001-15, presented at the 2001 SCA Symposium, Edinburgh, U.K.
[14] Tsimpanogiannis, I., N. and Yortsos, Y., C.: "The critical gas saturation in the presence of gravity", Journal of Coll. and Interf. Sc., vol. 270, 388-395, 2004.
[15] Nejad, K.S. and Danesh A., "Visual investigation of oil depressurisation in pores with different wettability characteristics and saturation histories", SPE 94054, Madrid, June 2005.

Tables and figures

Table 1

		Experiment 1 HK dry Berea 1m	**Experiment 2** HK dry Berea 10cm	**Experiment 3** LK P80	**Experiment 4** HK Swi Berea 44cm
Petro. parameters	Rock Type	Berea	Berea	P80	Berea
	L (cm)	89.9	9.8	30.7	44
	Kw (mD)	741.8	718.9	4.5	780.2
	Φ (%)	21.2	21.73	25.26	22.74
	Swi (%)	0	0	0	26.8
Sgc		3.3	3.6	12	7

Table 2

	High permeability exp 1&2		Low permeability exp 3		High permeability with water exp 4	
Simulation ID	**Sgc**	**N bub**	**Sgc**	**N bub**	**Sgc**	**N bub**
1	4.3	74	5.7	137	5.5	100
2	4.8	73	13.1	142	8.7	87
3	5.4	73	15.3	144	*5.2*	106
4	7.3	77	9.3	133	9.4	86
5	5.9	74	10.3	146	9.2	81
6	7.3	81	14.5	120	8.8	109
7	3.8	75	10.2	115	5.6	106
8	6.7	75	7.2	145	8.5	93
9	5.5	77	8.6	153	9.0	99
10	5.9	80	11.0	124	6.4	72
11	3.5	74	13.3	149	9.0	106
12	6.8	77	12.9	151	7.0	103
mean	**5.6**	**75.8**	**11.0**	**138.3**	**7.7**	**95.7**

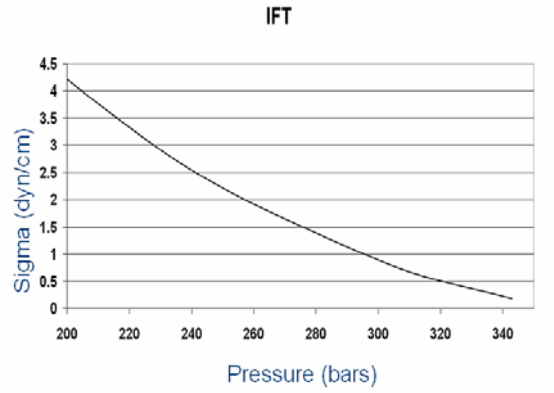

Fig 2: Evolution of the gas/oil interfacial tension

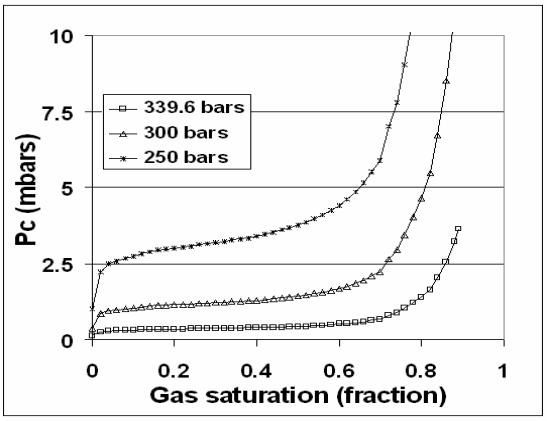

Fig 3: Evolution of Pc during depletion

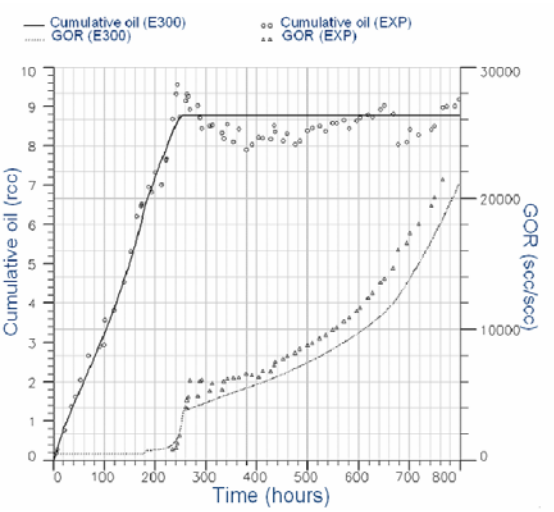

Fig 4: Cumulative oil production at reservoir conditions and GOR vs Pressure for Exp 1

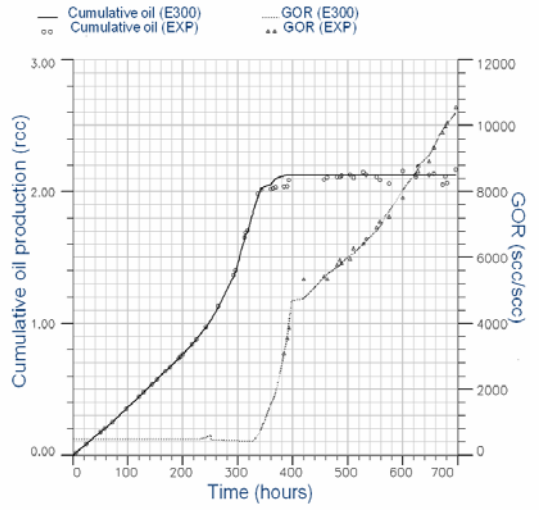

Fig 5: Cumulative oil production at reservoir conditions and GOR vs Pressure for Exp 2

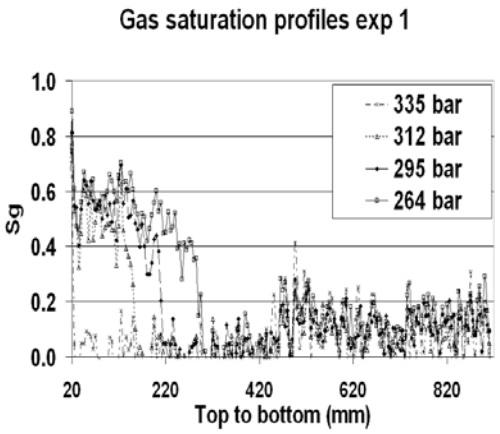

Fig6: In situ saturation profiles exp1

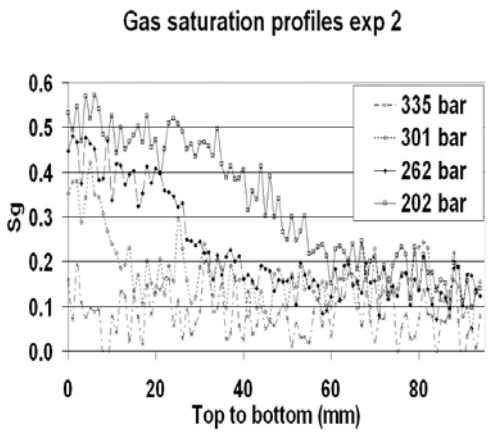

Fig7: In situ saturation profiles exp2

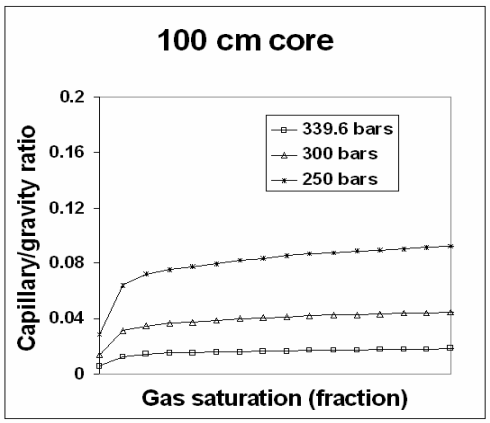

Fig8: Capillary/gravity ratio for the long core

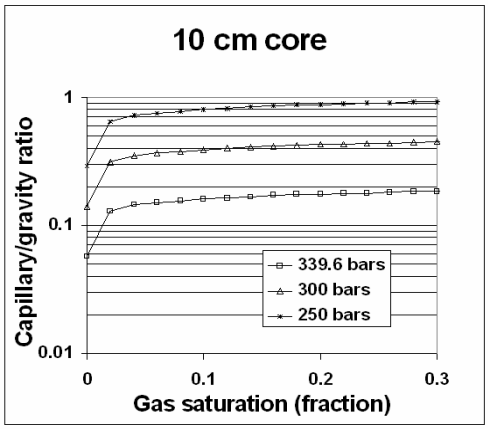

Fig9: Capillary/gravity ratio for the short core

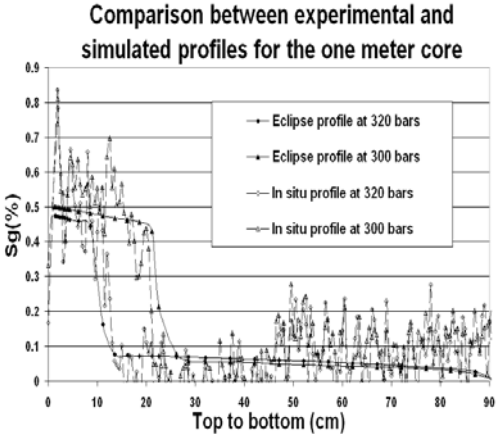

Fig10: History matching of in-situ saturation profiles for the 1m core

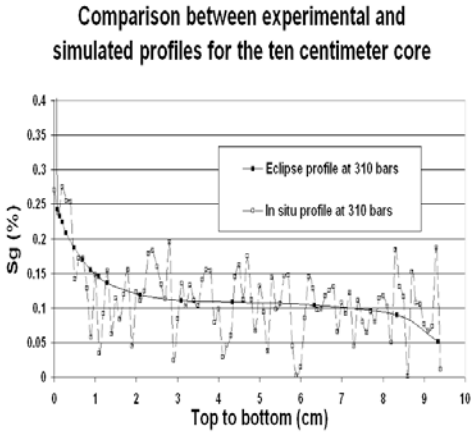

Fig11: History matching of in-situ saturation profiles for the 10cm core

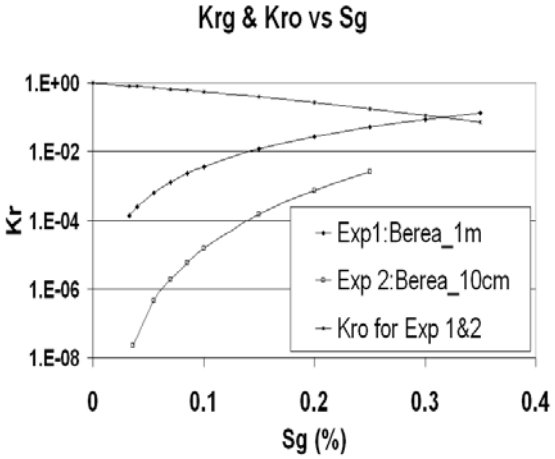

Fig12: Krg & Kro of Exp1&2 by hist. matching

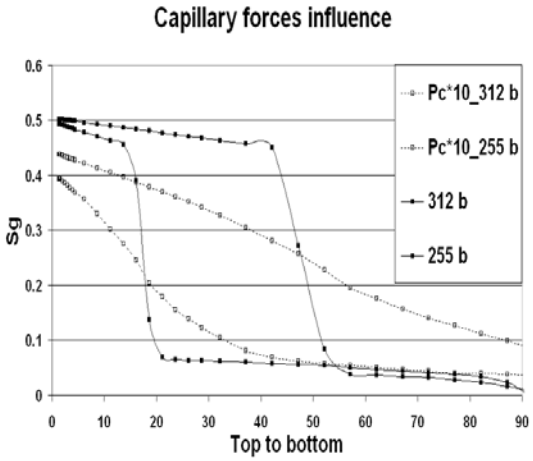

Fig13: Pc impact on saturation profiles

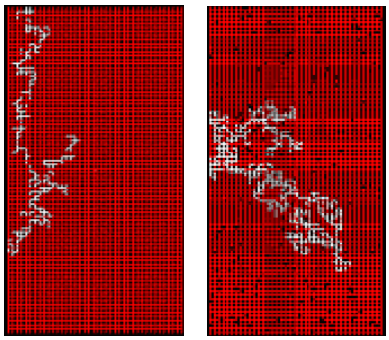

Fig14: PNM simulations of high (left) and low (right) permeability networks at Pb-P=950 psi

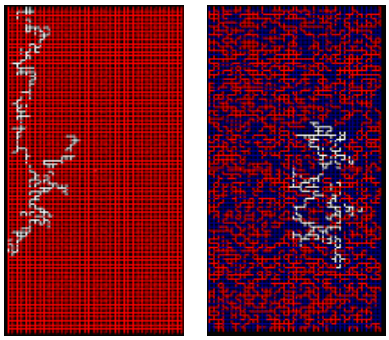

Fig15: PNM simulations of dry (left) and wet (right) networks at Pb-P=950 psi

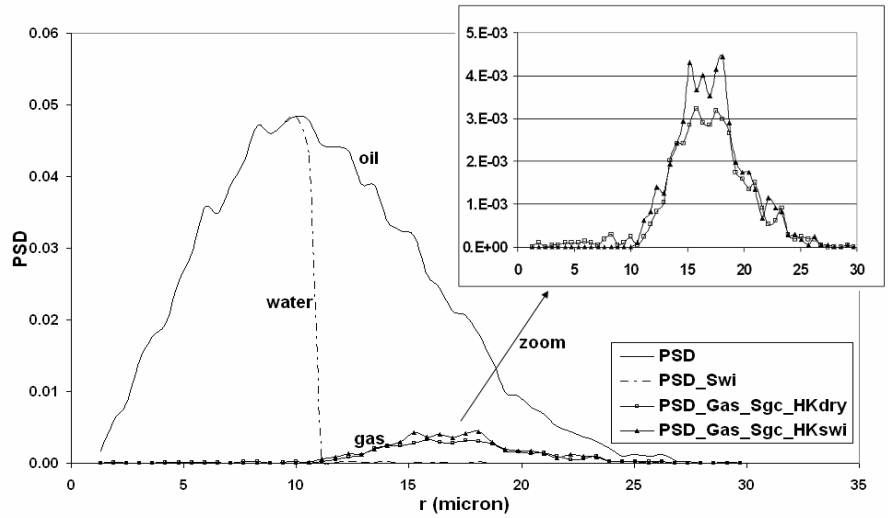

Fig 16: Gas pore occupancies at gas breakthrough for HK and HK Swi (Sim6) compared to overall distribution of oil and Swi (PSD=Pore Size Distribution)